

SOFI and ISAAC Pierce the Obscured Core of SBS 0335-052

L. VANZI, ESO, Chile; L. HUNT, CNR, Italy; T. THUAN, University of Virginia, USA

1. Introduction

In the list of Blue Compact Dwarf (BCD) galaxies known to date (Izotov & Thuan 1998, Kunth & Östlin 2000) SBS 0335-052 shows one of the lowest abundances, $Z = Z_{\odot}/41$, and is second only to I Zw 18 with $Z = Z_{\odot}/50$. Though new BCDs with low metallicity have been recently discovered (van Zee 2000, Kniazev et al. 2000), the two aforementioned galaxies keep holding the record. It is a general result that all star-forming low-metallicity galaxies are BCDs.

The study of such unevolved systems is extremely important to understand galaxy formation. It is believed that galaxies began to form at redshifts larger than 3 (Steidel et al. 1996) but all high- z galaxies discovered so far appear to be substantially enriched in heavy elements. Hence with these young nearby systems, we can study the star-formation process in environments which are sometimes much more pristine than those in known high-redshift galaxies. The star-formation process in primordial environments is very poorly understood but the metallicity obviously plays a fundamental role, nevertheless other parameters must be important as suggested by the variety of properties displayed by BCDs (Kunth & Östlin 2000).

SBS 0335-052 belongs to the handful of galaxies with abundance below $Z_{\odot}/20$ (Melnick et al. 1992), as such it is a candidate "local primordial galaxy" according to Izotov & Thuan (1999) who argued from the constancy of the N/O and C/O abundance ratios with O/H that galaxies with such low metallicity are younger than ~ 100 Myr. This idea however has been challenged by the recent observations of an evolved stellar population in I Zw 18 by Aloisi et al. (1999) and Östlin (2000).

HST observations of SBS 0335-052 have evidenced star formation occurring in six Super-Star Clusters (SSCs) not older than 25 Myr and located within a region smaller than 2 arcsec, or 520 pc at a distance of 54.3 Mpc (Thuan et al. 1997). Further observations obtained with ISO have shown a flux at $15 \mu\text{m}$ much brighter than expected and a spectral energy distribution that, at these wavelengths, is well

fitted by a highly absorbed modified black-body (Thuan et al. 1999 – hereafter TSM). From their fit, TSM deduce a visual extinction in the range 19–21 mag. and suggest that most of the star formation in SBS 0335-052 might be optically obscured. With this in mind we have started a programme aimed at a better understanding of the physical conditions in low-metallicity BCDs. In particular, the near-infrared (NIR) spectral region can help resolve the age controversy because of the uniformity of NIR colours in evolved stellar systems (Frogel 1985). Dust can be best targeted in the NIR, its thermal emission becoming evident above $2 \mu\text{m}$. The effects of extinction are reduced by roughly a factor of 10 in K band and by almost 20 in L band relative to the optical bands. Finally, NIR spectroscopy gives unique probes on the physics of the gas and constrains the star formation history of the galaxy through features like Br α , Br γ , H $_2$, [Fe II] and CO in absorption.

2. Observations

We have observed SBS 0335-052 on several occasions. Images in the J and Ks bands were obtained with SOFI at the NTT. These images were not very deep, only 300 sec. each, but had a good spatial resolution ($0.5''$). In addition we obtained a Ks image in the high-resolution imaging mode of SOFI during 400 sec. of integration; on this image we measure 0.3 arcsec seeing on a field star. This high-resolution image is shown in Figure 1 with the HST V contours overplotted. Previously we had obtained very deep exposures at UKIRT in J, H and K. The objective was to use the NIR colours to resolve the age issue since they are extremely effective indicators of stellar population ages and they allow to break the age-metallicity degeneracy when coupled with optical observations. However, colours of strong line-emitting galaxies are not representative of the stellar populations unless they are corrected

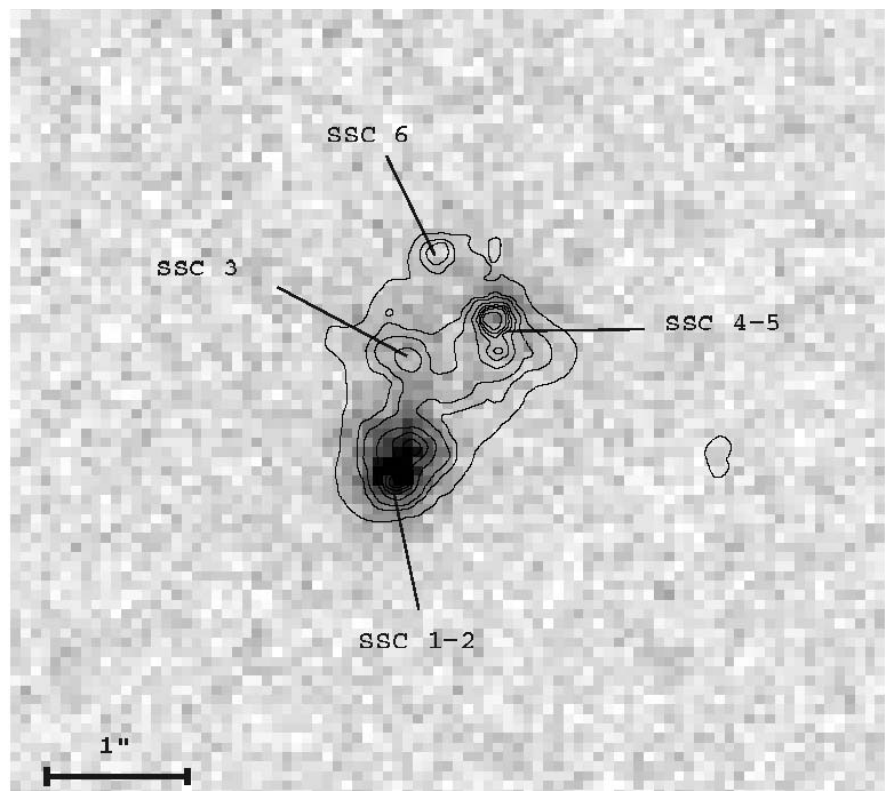


Figure 1: Ks image of SBS 0335-052 observed with SOFI at the NTT under $0.3''$ seeing. Contours in V band from the HST are overplotted.

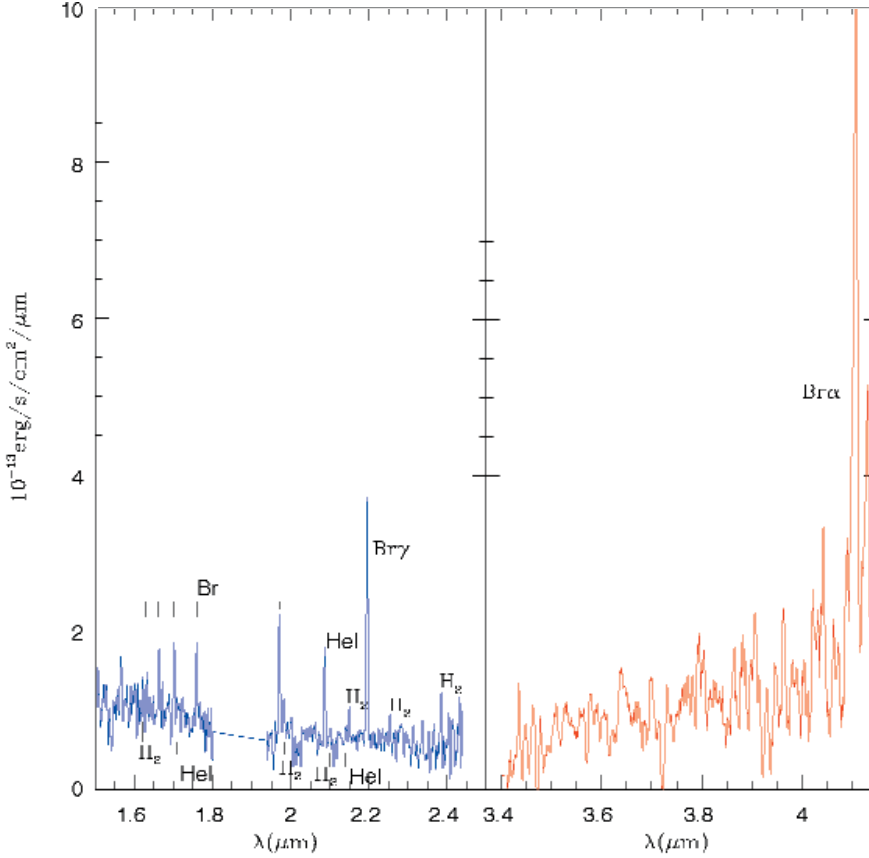


Figure 2: Low-resolution SOFI (blue) + ISAAC (red) infrared spectrum of SBS 0335-052.

for the nebular contribution. For this reason we also obtained a low-resolution spectrum ($R = 600$) covering the H and K NIR bands integrating 1 h 30 m and a medium-resolution ($R = 1400$) spectrum in the Ks band, 1 hour integration with SOFI at the NTT. The medium-resolution spectrum was observed under good seeing conditions ($0.5''$). In both cases we used a 1 arcsec wide slit and $PA = 145$. Finally, to better probe the high extinction found by TSM, we obtained a long wavelength ($2.7\text{--}4.2\ \mu\text{m}$) low resolution ($R = 360$) spectrum with ISAAC at the VLT-UT1 ANTU. A first observation with 30 minutes integration revealed a prominent $Br\alpha$ but with a too low S/N. Thanks to a Director discretionary time (DDT) approved programme we were able to integrate this first observation with 2 more hours of spectroscopy and a 30-minute L image before the galaxy set this year. Observations at these wavelengths are critical to probe the thermal regime and to check for the presence of dust and extinction. Figure 2 shows our low-resolution spectrum from 1.5 to $4.2\ \mu\text{m}$.

3. Results

3.1 Extinction

We measured the fluxes in the $Br\gamma$ and $Br\alpha$ recombination lines with an aperture of 1×1.5 arcsec. From Izotov et al. (1997) we have the flux in $H\alpha$ and $H\beta$ in the same aperture and can there-

fore attempt a multi-wavelength measure of the extinction by comparing the line ratios observed with the theoretical values. From the $Br\gamma$ measure, which was the first available to us, combined

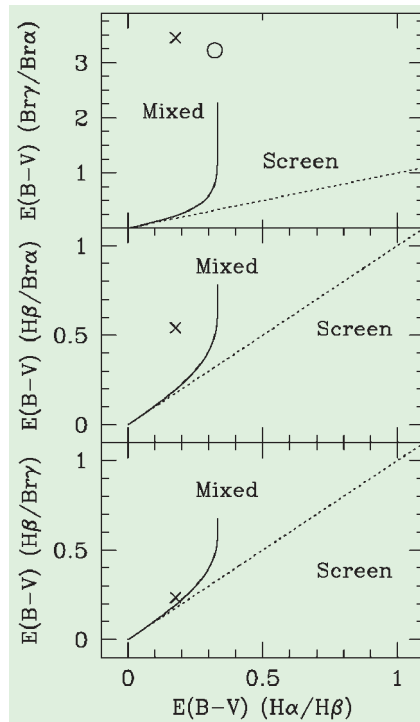


Figure 3: Colour excesses compared with a foreground screen and a mixed ISM. X is SBS 0335-052, O is NGC 5253.

Table 1: Values of the visual extinction measured with different recombination lines.

	$H\alpha/H\beta$	$Br\gamma/H\beta$	$Br\alpha/H\beta$	$Br\alpha/Br\gamma$
A_V	0.55	0.73	1.45	12.1

with $H\beta$, we obtained $A_V = 0.73$. This value was in agreement, within the errors, with the optical estimate of $A_V = 0.55$ showing little evidence, if any, for the heavily obscured star formation proposed by TSM. The recent measure of $Br\alpha$, however, gave a different result. Its comparison with $H\beta$ and $Br\gamma$ gives $A_V = 1.45 \pm 0.11$ and 12.1 ± 1.8 respectively. The values of optical extinction derived using different lines are summarised in Table 1. In Figure 3 we compare the corresponding values of $E(B-V)$ with a foreground screen of dust and a homogeneously mixed medium of dust and gas. Neither model gives an adequate description of the observations, although the mixed model is a better representation. Since the optical lines give very low extinction, a more likely picture consists of a dust free region responsible for most of the optical emission surrounding a highly obscured central core. In Figure 3 we also show the point corresponding to the blue dwarf galaxy NGC 5253 considered by Rieke et al. (1988) to be the youngest starburst known.

3.2 Stellar Population

Our NIR images achieve a spatial resolution that almost matches HST; in particular the regions corresponding to the SSC 1+2 and 4+5 are clearly resolved. Combining the NTT and HST images we have been able to build an optical-NIR colour-colour diagram including different regions of the galaxy. In Figure 4 we plot the points corresponding to the SSC 1+2 and 4+5, the global emission (E) and the north-west extended component (Ex) of the galaxy. The green solid line is the output of Leitherer et al. (1999, SB99) for a metallicity $Z_{\odot}/20$. Though SB99 includes the contribution of the nebular continuum emission, it does not reproduce the colours observed. This can be due to different reasons: (1) the metallicity of SBS 0335-052 is significantly lower than the model; (2) the high contribution of the emission lines to the broadband magnitudes. To investigate this we constructed a new model using the stellar SED for $Z_{\odot}/50$ – blue dotted line – and including nebular continuum and emission lines (see Vanzì et al. 2000 for details). The blue dots of Figure 4 correspond to ages of 3 and 5 Myr for this new model with the gas contribution included. The colours of the SSC 1+2 and 4+5, though not perfectly, are better reproduced than with SB99 and are consistent with a very

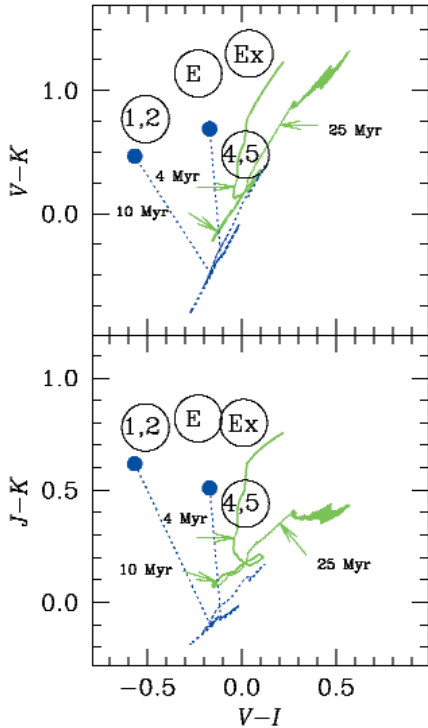


Figure 4: Optical-NIR colour-colour diagram of different regions in SBS 0335-052, mainly SSC1+2, 4+5, the whole galaxy (E) and north-west extended region (Ex). The green curves are the SB99 model with 4, 10 and 25 Myr indicated by arrows. Blue dotted curves represent the colours of a $Z_{\odot}/50$ stellar population, dotted lines connect the points of age 3 and 5 Myr to the points that include the nebular contribution.

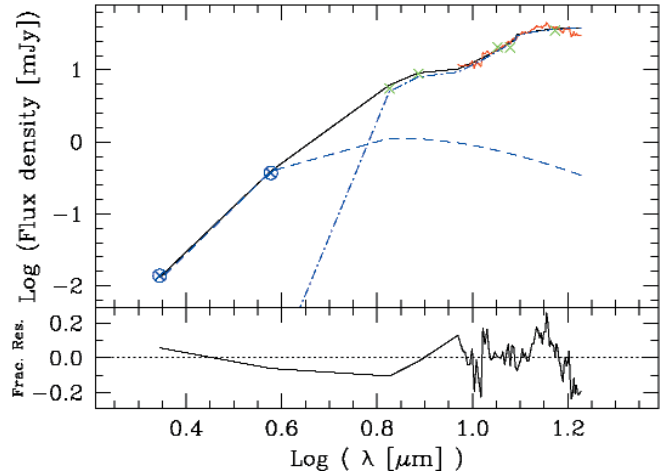
young population. Neither globally nor in the extended emission down to 23 K-mag/arcsec² do we find evidence for an evolved population. By including the colours of an evolved population in the model we can estimate what fraction of old stars can be present. Since we detect no evolved stars in our observations, the limit is set by the photometric errors and turns out to be $\sim 15\%$. This finding is supported by the non-detection of stellar absorption features in our NIR spectra. Though the S/N ratio on the continuum is never higher than 5, the CO bands at 2.3 μm should be prominent and observable if a population older than 10 Myr were dominating the K continuum. However, the non-detection of CO in absorption could also be attributed to the low metallicity of the galaxy.

We detect the helium recombination lines $4^3\text{D} - 3^3\text{P}^0$ at 1.700 μm and the blend of $4^1\text{S} - 3^1\text{P}^0$ and $4^3\text{S} - 3^3\text{P}^0$ at 2.113 μm . Their intensities relative to Br10 and Br γ respectively are consistent with the presence of stars more massive than 35 M_{\odot} (Vanzi et al. 1996, Vanzi et al. 2000) and therefore with the very young age of the galaxy.

3.3 Dust and Gas Content

The presence of dust in SBS 0335-052 has been inferred directly through

Figure 5: Fit of the IR SED. The green crosses are the photometric points from ISO, the blue circled crosses are the measures from SOFI and ISAAC and the red spectrum is from ISO. The blue dashed lines represent the modified black bodies and the dark line the best fit to all observations. In the lower panel the fitting residuals are displayed.



infrared observations, it is the only BCD observed in the mid-infrared along with He 2-10 (Sauvage et al. 1997) whose metallicity is not as extreme. The K-L colour is unusually red for a non Seyfert galaxy and has an average value of about 2. In Figure 5 we show the IR Spectral Energy Distribution built from the ISO observations of TSM and our K and L points after correcting for nebular and stellar emission. The data have been fitted by the superposition of two modified black bodies, one with $T = 192$ K obscured by $A_V = 16$ and the other with $T = 459$ K and no extinction. From the extinction observed we derived a total amount of dust of about $5 \cdot 10^3 M_{\odot}$. Such an amount would not have been expected in a BCD, but it is consistent with the expected production of type II supernovae. From the Br α flux and using the starburst model of Rieke et al. (1993) we derive a SN rate of about $6 \cdot 10^{-4} \text{ yr}^{-1}$ that, integrated over the present burst lifetime after onset of SN, gives about $2 \cdot 10^3$ SN. Each massive SN is expected to produce about 1 M_{\odot} (Todini & Ferrara 2001) which would produce about $2 \cdot 10^3 M_{\odot}$ of dust, roughly consistent with what is observed.

For what concerns the gas, most BCDs are undetected in the CO (1-0) transition (Taylor et al. 1998). This finding contrasts with the relative brightness of these objects in HI at 21cm (Thuan et al. 1999) and was initially interpreted as due to the

large ratio of neutral to molecular gas produced by the unusually high star-formation efficiency of these galaxies. However, recent evidence suggests a high H_2/CO ratio rather than a molecular gas deficiency (Taylor & Klein 2001). Our H_2 detection in the NIR spectrum of SBS 0335-052 supports the idea that molecular gas is actually present in BCDs though difficult to detect in the CO. At least 4 H_2 lines are clearly detected in our K spectrum. The comparison of the relative strength of these lines with the models support UV fluorescence as the main excitation mechanism.

3.4 Star Formation and Geometry

Our medium-resolution 2 μm SOFI spectrum was acquired under very good seeing conditions. The spatial profile of the emission lines is similar, and clearly distinct from the continuum. While Br γ and H_2 have a single-peaked spatial profile, the continuum shows a double peak. This is clearly shown in Figure 6. The main peak of the continuum and the emission lines are spa-

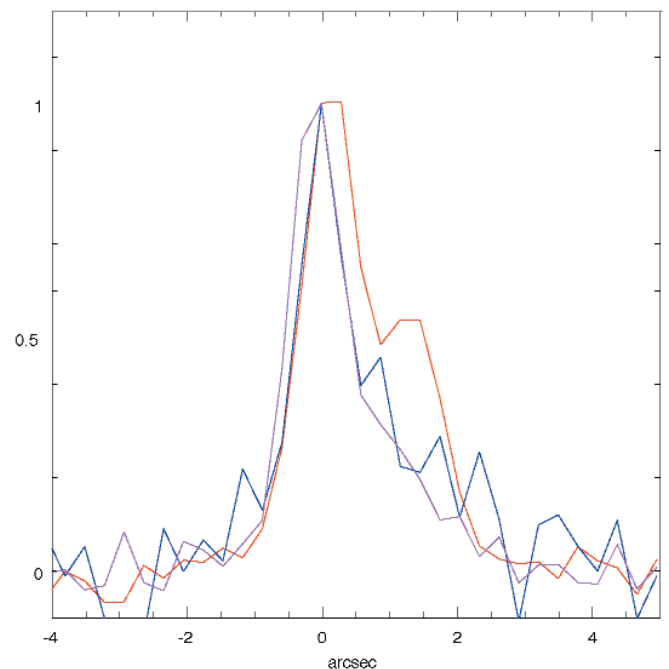


Figure 6: Spatial profile of Br γ – magenta – H_2 – blue, and 2 μm continuum – red.

tially shifted by about 60 pc meaning that the site of the most recent star formation is not located at the peak of the continuum. The same is detected by Izotov et al. (1997) in the optical but, in this case, the spatial shift is larger and about 200 pc. We interpret this as due to the larger contribution from the ionised gas to the NIR continuum than to the optical one, but it could also be partly an effect of extinction.

The L image, observed at the VLT with 0.5" seeing, reveals a very compact source at the position of the SSC 1+2. It is difficult to compare the location of this object with respect to the spectral profiles due to the lack of a reference point in the latter but, on the basis of this observation and the extinction derived at different wavelengths, we can envision the following picture.

Star formation occurs in a heavily obscured central core that contributes most of the IR emission. This core lies behind a dust-free region that instead emits the bulk of the optical radiation observed. The central burst produced a number of supernovae that polluted the interstellar medium with dust. Assuming that all the H α flux observed

is generated in the external shell and using standard line ratios we derive that the outer region contributes 50% of Br γ and only 25% of Br α . In other words, 75% of the star formation in SBS 0335-052 is only observable at 4 μ m! (see Hunt, Vanzi & Thuan 2001 for details). These results open a new view on SBS 0335-052 and possibly on star formation at high redshift. If the hidden star formation in SBS 0335052 is typical of young galaxies at high redshifts, then the cosmic star formation rate as derived from UV-optical observations would be underestimated by a factor 2–3. ISO surveys of distant galaxies (Flores et al. 1999) suggest that this is the case.

References

- Aloisi, A., Tosi, M., Greggio, L. 1999, *AJ*, **118**, 302.
 Flores H., Hammer F., Thuan T.X., Cesarsky C. et al. 1999, *ApJ* **517**, 148.
 Frogel J. 1985, *ApJ* **298**, 528.
 Hunt L.K., Vanzi L., & Thuan T.X. 2001, *A&A*, submitted.
 Izotov Y.I., Thuan T.X. 1998, *ApJ* **500**, 188.
 Izotov Y.I., Thuan T.X. 1999, *ApJ* **511**, 639.

- Izotov Y.I., Lipovetsky V.A., Chaffee F.H. et al 1997, *ApJ* **476**, 698.
 Leitherer C., Schaerer D., Goldader J.D. et al. 1999, *ApJS* **123**, 3.
 Kniazev A.Y., Pustilnik S.A., Masegosa J., Marquez I. et al. 2000, *A&A* **357**, 101.
 Kunth & Östlin 2000, *A&A Rev.* **10**, 1.
 Melnick J., Heydari-Malayeri M., Leisy P. 1992, *A&A* **253**, 16.
 Östlin, G. 2000, *ApJ* **535**, L99.
 Rieke G.H., Lebofsky M.J., Walker C.E. 1988, *ApJ* **325**, 687.
 Rieke G.H., Loken K., Rieke M.J., Tamblyn P. 1993 *ApJ* **412**, 111.
 Sauvage M., Thuan T.X., Lagage P.O. 1997, *A&A* **325**, 98.
 Steidel C.C., Gialalisco M., Pettini M., Dickinson M., Adelberger K.L. 1996, *ApJ* **462**, L17.
 Taylor C.L., Kobulnicky, H.A., Skillman E.D. 1998 *AJ*, **116**, 2746.
 Taylor C.L., Klein U. 2001, *A&A* **366**, 811.
 Thuan T.X., Izotov Y.I., Lipovetsky V.A. 1997, *ApJ* **477**, 661.
 Thuan T.X., Sauvage M., Madden S. 1999, *ApJ* **516**, 783.
 Thuan T.X., Lipovetsky, V.A., Martin J.M., Pustilnik S.A. 1999 *A&AS* **139**, 1.
 Todini P., Ferrara A. 2001, *MNRAS*, submitted.
 van Zee L. 2000, *ApJ* **543**, L31.
 Vanzi L., Rieke R.H., Martin C.L., Shields J.C. 1996, *ApJ* **466**, 150.
 Vanzi L., Hunt L.K., Thuan T.X., Izotov Y.I. 2000, *A&A* **363**, 493.

Eigenvector 1: An H-R Diagram for AGN?

J. W. SULENTIC¹, M. CALVAN², P. MARZIAN²

¹Department of Physics and Astronomy, University of Alabama, Tuscaloosa, AL, USA

²Osservatorio Astronomico di Padova, Padova, Italy

Abstract

Observations with 1.5-m-class ESO telescopes have contributed significantly to a much clearer understanding of the phenomenology of Active Galactic Nuclei (AGN) that has emerged over the past seven years. Long-slit spectra of good resolution and high S/N enable us to accurately measure emission-line parameters for a significant number of AGN. Combined with soft X-ray and UV line measures from Hubble Space Telescope, the data reveal a parameter space that distinguishes between the diverse classes of AGN and organises them in a way that promises to redefine the input to physical models. We suggest that this Eigenvector 1 (E1) parameter space may be as close as we will ever come to finding an H-R diagram for quasars. Several arguments suggest that the ratio of AGN luminosity to black hole mass ($L/M \propto$ accretion rate) convolved with the effects of source orientation drives the principal E1 correlation. While L/M sustains, in a sense, the H-R analogy beyond phenomenology, the

role of orientation reflects the greater complexity inherent in the lack of spherical symmetry for AGN.

1. Introduction

The H-R Diagram is well known as the most fundamental correlation space for stars. A plot of surface temperature vs. luminosity effectively discriminates between the diversity of normal and "abnormal" stellar types. Main-sequence stars show a strong correlation in the space while stars in other evolutionary stages are identified by their different domain space occupation. The fact that a 2-D correlation space is so effective reflects the simplicity of the law of hydrostatic equilibrium that governs stellar structure. Thus the principal driver of the correlation space is stellar mass. It is possible that after less than 50 years of study we might see a similar correlation space on the horizon for Active Galactic Nuclei (AGN). ESO spectroscopic observations have made a significant contribution to the work that has led to the Eigenvector 1 concept. The fundamental parameters of

an AGN correlation space might be expected to be more numerous than those for a stellar diagram because we are observing a combination of primary continuum and secondary line and continuum emission components in a structure with complex geometry. In fact, the 2-D optical (for low z quasars) parameter plane reveals much of the correlation power. In its present evolution our 4-D Eigenvector 1 correlation space shows a phenomenological discrimination in several ways comparable with that of the H-R diagram for stars. The veracity and implications of that statement will likely be the subject of much research in the next decades.

A defining characteristic of AGN involves the presence of broad emission lines (usually FWHM H $\beta \geq 10^3$ km/s). This definition encompasses Seyfert 1 nuclei, QSO's, broad line radio galaxies and quasars. BLLACs (in low continuum phase) and Seyfert 2 nuclei (in polarised light) also sometimes show broad lines. Although the first AGN (quasars) were discovered because of their radio-loudness, it is now known that the bulk of AGN are radio-quiet.